Fluid Dynamics & Materials Processing

Tech Science Press

DOI: 10.32604/fdmp.2021.014290

ARTICLE

Macromolecule's Orientation in a Nanofiber by Bubble Electrospinning

Dan Tian[1,*], Danni Yu[2] and Chunhui He[3]

[1]School of Science, Xi'an University of Architecture and Technology, Xi'an, 710055, China

[2]National Engineering Laboratory for Modern Silk, College of Textile and Clothing Engineering, Soochow University, Suzhou, China

[3]School of Civil Engineering, Xi'an University of Architecture & Technology, Xi'an, 710055, China

[*]Corresponding Author: Dan Tian. Email: tiandan@xauat.edu.cn

Received: 15 September 2020 Accepted: 07 February 2021

ABSTRACT

In the search for sustainable alternatives to harmful synthetic fibers, an increasing amount of research focuses on biomimicry and natural fibers. Sea silk is an exceptional textile material. It is a kind of natural silk produced using the long silky filaments secreted by a specific bivalve mollusk (*Pinna nobilis*); now at edge of extinction. This paper suggests a simple but effective way to prepare artificial sea silk from *Mytilus edulis*. A sea silk solution is prepared using a *Mytilus edulis* protein, and a polyvinyl alcohol (PVA) solution is mixed with the sea silk solution in order to produce artificial sea silk through a bubble electrospinning technique. The effects of the sea silk concentration on the nanofiber's morphology and mechanical properties are studied experimentally.

KEYWORDS

Mollusk; sea-silk solution; collagenous fibers; bubble electrospinning

1 Introduction

Natural silks, like spider silk and silkworm silk, have been extensively studied throughout the literature due to their sustainable production, mechanical characteristics and biofriendly nature [1,2]. According to the principle of spider spinning, we designed a new electrospinning [3–5]. Zhou et al. [6] combined the silkworm and electrospinning. Yu et al. [7,8] used the snail and spider in electrospinning and prepared the nanofibers with outstanding properties. Nevertheless, none of the above examples have exploited the power of nature to produce this incredible variety of high-performance materials in a very clean and efficient manner. Nature offers a wide range of highly adapted solutions that have inspired and continue to inspire the development of a wide range of man-made materials, devices and tools. Among natural silks, the sea silk has been ignored by the whole academic community. Sea silk is one of the oldest natural silks with a history of more than 5000 years [9–11], but the entire scientific community has not paid any attention to the fabrication of sea silk. Although, the news media has produced a series of intensive reports on this extraordinary natural material. The natural collagenous fibers were produced from mollusc, mainly from *Pinna nobilis* in the Mediterranean region. The natural silk has many fascinating properties like extremely light weight and remarkable flexibility, good anti-microbial barrier, high abrasion resistance, excellent shock-absorbing property, astonishing self-healing capacity, and golden shinning when exposed to the sunlight [12–17].

The technology for weaving sea silk cloth is extremely intricate [6], and this kind of textile heritages has been abandoned. According to BBC news [7–9], there exists only an old woman in an Italian island who can make sea silk, and the technology will be soon become myths and legends though there are many records in the history. For example, it was recorded in New Book of Tang (新唐书), a historical work about the imperial Tang dynasty of China. Literally the water wool (sea silk) was wove to cloth, which was called as Western Sea Cloth. In addition, factors such as the viscosity of the spinning solution have an impact on some properties of the prepared materials [18–20]. A fisherman sails to coral reefs in sea to harvest mussels. Byssal threads are attached to stones, and it is white at initial stage, but it will become different color after many years.

In order to make the forgotten textile technology alive, we collect *Mytilus edulis* to produce artificial sea silk instead of the endangered *Pinna nobilis*. The former has been intensely commercially used and massively and intensively cultivated [18], while the latter is now an endangered species [21–25]. The bubble electrospinning [26–28] was adopted in this paper to fabricate artificial sea-silk.

2 Materials and Methods

2.1 Materials

Polyvinyl alcohol (PVA) with Alcoholysis degree of 97.5–99.0 mol% (Shanghai Aladdin Biochemical Technology Co., Ltd., Shanghai, China), and used without purification.

Mytilus edulis (Fig. 1) was purchased from Zhoushan Islands, China. Its whole meat weighted 118.63 g was used for preparation of the needed sea-silk solution by putting it into an alcohol solution with mass of 177.345 g and stirring the mixture for 2 h until the solution become homogeneous, then using a filter screen (500 mesh) to filter the solution, the weight of the remnants was 31.16 g. Finally, we stored the solution in a refrigerator at 0°C.

Figure 1: *Mytilus edulis*

2.2 Solution Preparation

8 wt% PVA solution was prepared first, then mixed it with sea-silk solution with different concentrations, see Tab. 1. The blended solution was magnetically stirred (DF-101S, Xinrui instrument Inc., Beijing, China) under the temperature of 80°C. Before the spinning process, the spun solution was further ultrasonically treated using an ultrasonic cleaner (SL-5200DT, Nanjing Shunliu Instrument Co., Nanjing, China) for 2 h to guarantee complete dispersion of sea-silk solution in the spun solution.

Bubble electrospinning [23–25] was used in our experiment, the experiment setup was illustrated in Fig. 2. On the surface of the solution, bubbles were produced, which were further stretched by the electrostatic force until rupture, multiple jets with a high velocity of more than 100 m/s were ejected to form nanofibers. The outstanding advantage of the bubble electrospinning is the high output of nanofibers.

Table 1: Each sample's components and properties of fiber membrane

Samples	PVA/Sea silk	Average diameter (nm)	Thickness (mm)	Maximal stress (Mpa)	Energy absorbing (J)	Contact angle (degree)
1	1:0	127	0.091	0.976	1.492	6.6
2	2:1	254	0.06	4.356	7.560	36.7
3	1:1	176	0.07	6.261	5.828	25.2
4	1:2	171	0.068	5.102	9.855	30.6

The diameter of the nozzle was 4 cm, regulated the voltage to 40 kV, the temperature to 18.8°C, and relative humidity to 48%, the distance between the nozzle and collector to 26.5 cm.

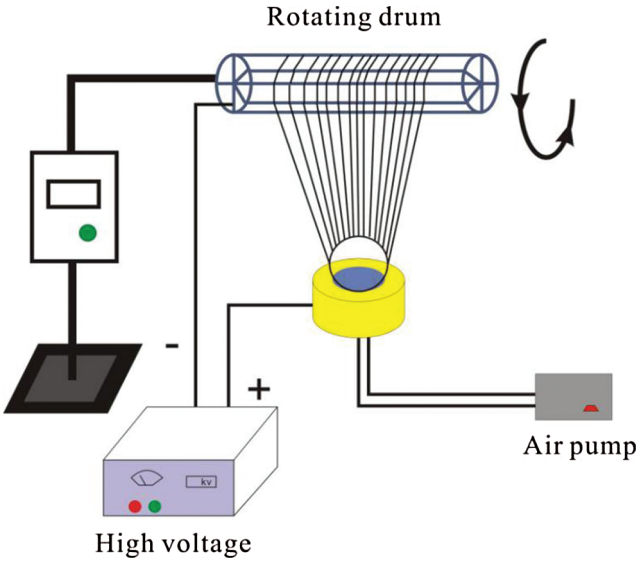

Figure 2: Bubble electrospinning

2.3 Instrumentation

Nanofiber's morphology was obtained via a S4800 Cold Field Scanning Electron Microscope (SEM, Hitachi S-4800, Tokyo, Japan). Nanofiber's diameter distribution was measured by ImageJ Software (National Institute of Mental Health, Bethesda, Maryland, USA). Mechanical property was analysed by INSTRON-3365 Material Testing Machine (INSTRON Company, USA). Contact angle (CA) was measured via Krüss DSA 100 apparatus (Krüss Company, Germany). Raman spectrum was measured via Raman spectrometer (LabRAM XploRA).

3 Results and Discussion

3.1 Morphological Characterization (SEM)

The SEM images are shown in Fig. 3. We can see that the addition of the sea silk solution in the polymer solution results in larger nanofiber diameter than that of the PVA nanofibers, see Fig. 4 and Tab. 1, however a higher sea silk concentration produces smaller fibers.

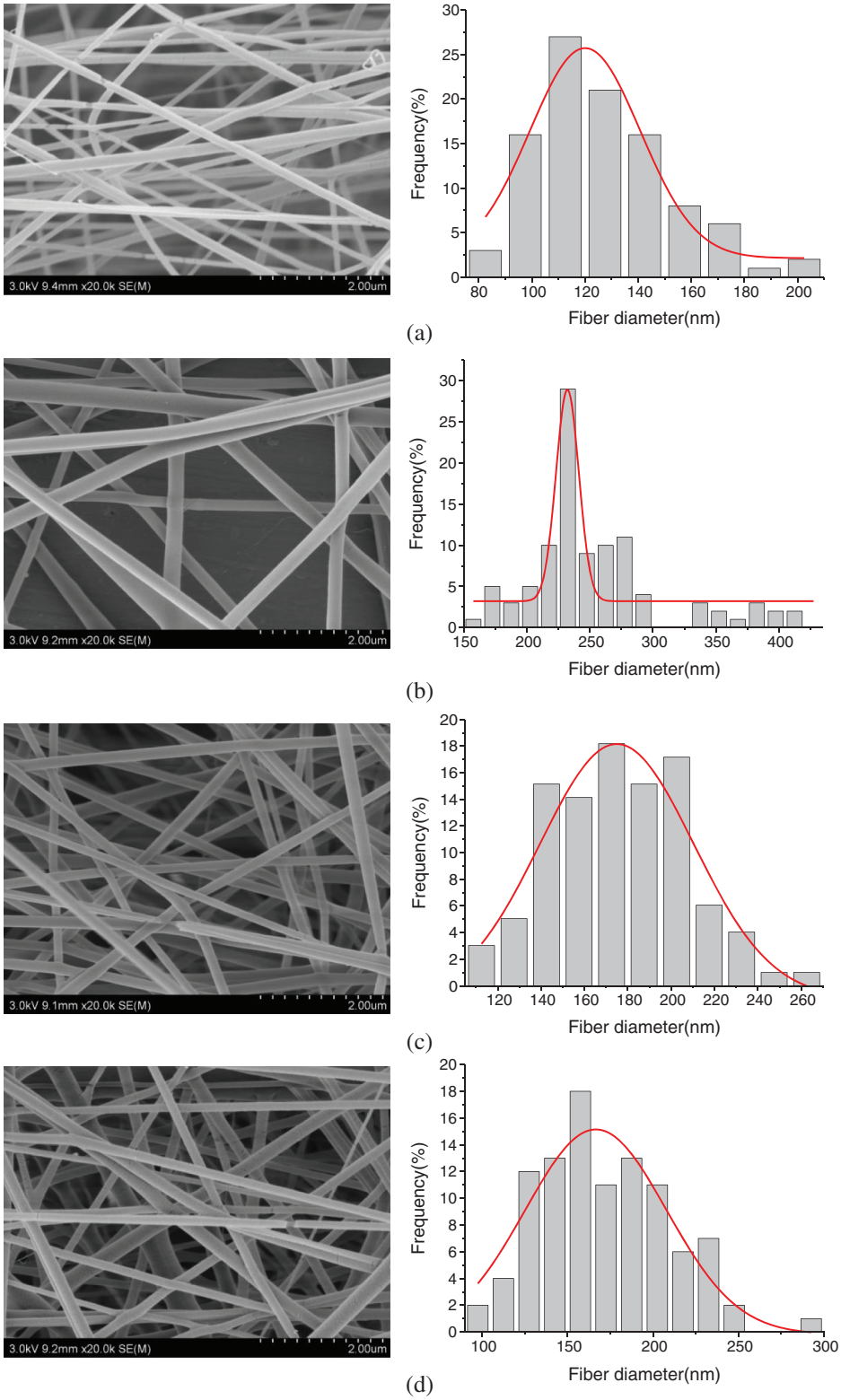

Figure 3: SEM illustrations for each sample. (a) sample 1: PVA/Sea silk = 1:0, (b) sample 2: PVA/Sea silk = 2:1, (c) sample 3: PVA/Sea silk = 1:1, (d) sample 4: PVA/Sea silk = 1:2

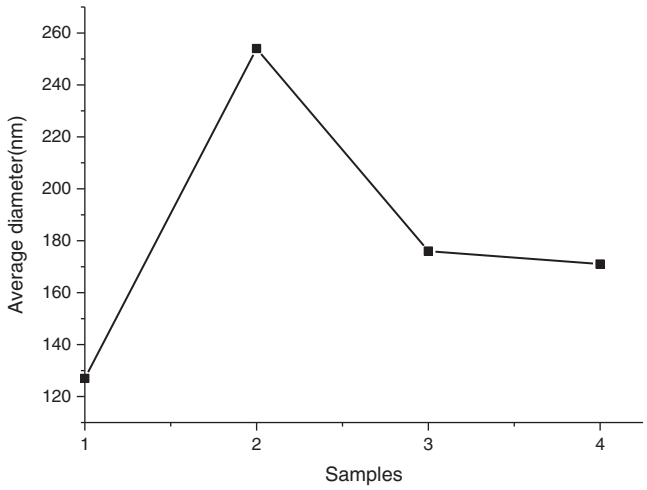

Figure 4: Average diameters of different sample

This is because that the *Mytilus edulis*' protein involved in the sea silk solution has an intrinsic property of fast solidification. After starting electrospinning, the curing speed of sea silk solution is much faster than that of PVA, and the cured protein prevents the solution from flowing in the nozzle, resulting in an increase in diameter. However, the fiber's diameter reduces with the increase of the sea silk concentration. This can be explained using continuity equation in fluid mechanics.

In the electrospinning process, the continuity equation for one-dimensional moving jet can be expressed as

$$A\rho u = Q \tag{1}$$

where u is the velocity of the jet, ρ is the density of the jet, A is the area of the jet cross section, and Q is the constant flow ratio.

The spinning solution can be roughly regarded as a two-phase flow of sea silk solution and PVA solution.

Each component follows the following continuity equation

$$A_1\rho_1 u = Q_1 \tag{2}$$

$$A_2\rho_2 u = Q_2 \tag{3}$$

where subscripts 1 and 2 imply the PVA solution and the sea silk solution, respectively. The components satisfy the following identity relations

$$Q_1 + Q_2 = Q \tag{4}$$

$$A_1 + A_2 = A \tag{5}$$

$$\rho = c_1\rho_1 + c_2\rho_2,\ c_1 + c_2 = 1 \tag{6}$$

where c_1 and c_2 are respectively the concentrations of the PVA solution and the sea silk solution.

Eq. (1) can be written in the equivalent form

$$(A_1 + A_2)(c_1\rho_1 + c_2\rho_2)u = Q \tag{7}$$

From Eqs. (2) and (3), we have

$$A_1 = \frac{Q_1\rho_2}{Q_2\rho_1}A_2 \tag{8}$$

Substituting Eq. (8) into Eq. (7), we have

$$(\frac{Q_1\rho_2}{Q_2\rho_1} + 1)A_2(c_1\rho_1 + c_2\rho_2)u = Q \tag{9}$$

Solving the equation, we have

$$A_2 = \frac{Q_2\rho_1 Q}{u(Q_1\rho_2 + Q_2\rho_1)(c_1\rho_1 + c_2\rho_2)} = \frac{Q_2\rho_1 Q}{u(Q_1\rho_2 + Q_2\rho_1)(\rho_1 + c_2(\rho_2 - \rho_1))} \tag{10}$$

In our experiment, $\rho_2 > \rho_1$, Eq. (10) predicts a smaller jet section (large value of A_2 or A) or equivalently a smaller fiber diameter for a higher concentration of the sea silk solution (a larger value of c_2), this prediction agrees with the experimental observation as illustrated in Fig. 4.

3.2 Mechanical Properties Analysis

The mechanical properties of the samples are shown in Fig. 5. The maximum stresses of the four samples were, respectively, 0.976 Mpa, 4.356 Mpa, 6.261 Mpa, and 5.102 Mpa. The energy-absorbing property depends upon the strain energy, which corresponds to the area under the stress-strain curve, the values for 4 samples are respectively 1.492, 7.560, 5.828, and 9.855.

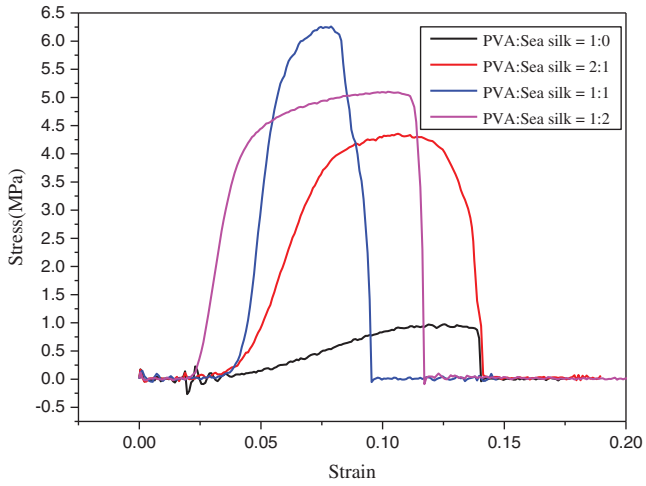

Figure 5: Stress–strain curve

Obviously, the addition of silk solution can greatly improve the mechanical properties of nanofibers, which benefits from natural silk's property, the strength of a byssus is higher than that of a metal wire with same diameter.

According to the nano effect [29], the maximal stress can be expressed in the form

$$\sigma = \sigma_0 + \frac{k_\sigma}{D^\alpha} \tag{11}$$

where D is the average diameter of the obtained fibers, σ is the maximal stress, σ_0 is its bulk's property, in this paper σ_0 is the maximal stress for the pure PVA fibers, k_σ is a material constant, α is a scaling parameter, we always choose $\alpha = 1/2$ for qualitative analysis.

Comparison between Sample 2 and Sample 3 results in

$$\frac{\sigma_3 - \sigma_0}{\sigma_2 - \sigma_0} = \left(\frac{D_2}{D_3}\right)^{1/2} = \left(\frac{254}{176}\right)^{1/2} = 1.20 \tag{12}$$

while its experimental value is

$$\frac{\sigma_3 - \sigma_0}{\sigma_2 - \sigma_0} = \frac{6.261 - 0.976}{4.356 - 0.976} = 1.56 \tag{13}$$

Its prediction accuracy is about 30%. The error arises in many factors including fiber's diameter distribution and the value of α.

3.3 Wetting Properties

Fig. 6 shows the wettability of samples. After adding the sea silk solution, the wettability of nanofibers has a big change. The contact angle depends upon fiber's diameter, according to Liu et al. [30], the contact angle scales with the fiber diameter in the form

$$\theta \propto D^{\beta} \tag{14}$$

where β is the value of the fractal dimensions of the membrane's surface $0 < \beta < 2$. Eq. (14) predicts a smaller contact angle for smaller fibers, this agrees with our experiment data, see Fig. 6.

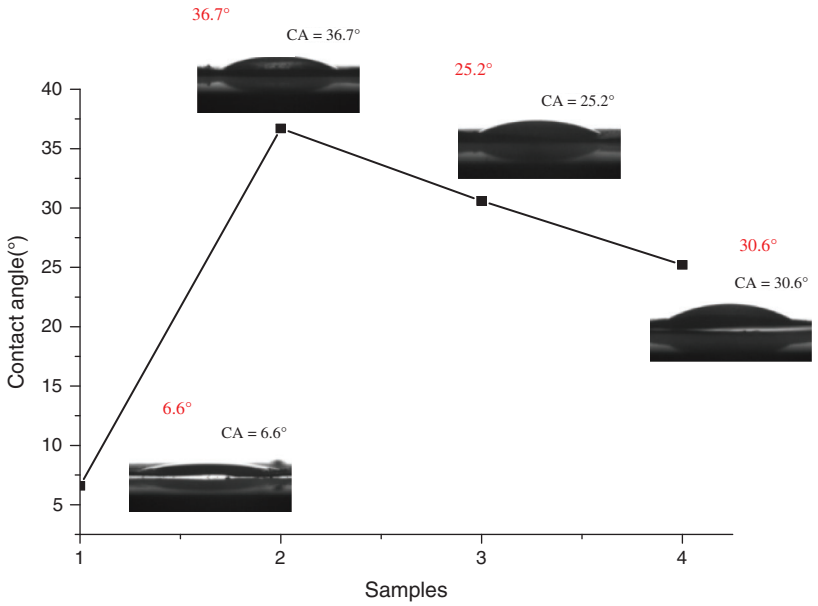

Figure 6: Wetting property of each sample

3.4 Raman Analysis

The sea-silk solution exhibits two peaks at 1459 cm^{-1} and 2929 cm^{-1}, respectively, the artificial sea-silk membrane also exhibits the same peaks, see Fig. 7, revealing that the sea-silk solution is well incorporated into the artificial sea-silk.

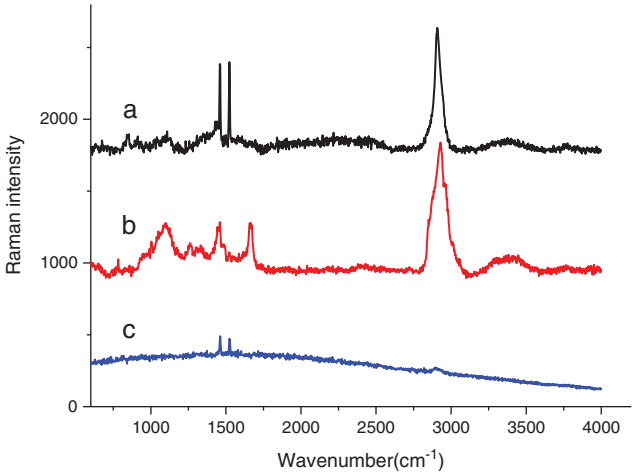

Figure 7: Raman spectra of (a) the sea-silk/PVA membrane, (b) sea-silk solution, and (c) PVA membrane

4 Conclusions

Natural fibers have an important role to play, among which *P. nobilis* byssus fibers are especially fascinating due to their conventional use as precious, light and warm clothing material on the one hand and as a motivation for the creation of new green materials due to its significant mechanical properties on the other hand. The protein involved in the sea-silk solution has greatly affected on the spinning process, nanofiber's morphology, nanofiber's mechanical properties and nanofiber's wetting property. Due to the addition of sea silk, the mechanical properties of nanofibers are significantly improved, and the water contact angle of nanofibers becomes larger than pure PVA nanofibers. The natural sea-silk has many fascinating properties, and this paper is a first step to inspire new strategies for making the natural silk alive. This preliminary study still leaves much space to further research on the artificial seal-silk's other properties such as anti-microbial property, abrasion, shock-absorb ability and self-heal capacity. The potential applications of this mussel-inspired fibers might give a far-reaching influence on textile engineering and biomaterials.

Funding Statement: This work was supported by the Foundation of Xi'an University of Architecture and Technology in 2020 [Tian Dan]; The Natural Science Foundation of Shaan Xi Province in 2019 [2019JQ-755]; and the Natural Science Foundation of Shaanxi Provincial Department of Education in 2019 [19JK0462].

Conflicts of Interest: The authors declare that they have no conflicts of interest to report regarding the present study.

References

1. Johari, N., Hosseini, H. R. M., Samadikuchaksaraei, A. (2018). Novel fluoridated silk fibroin/TiO_2 nanocomposite scaffolds for bone tissue engineering: C. *Materials Science and Engineering, 82(41),* 265–276. DOI 10.1016/j.msec.2017.09.001.
2. Xing, C., Munro, T., Jensen, C., Ban, H., Copeland, C. G. et al. (2017). Thermal characterization of natural and synthetic spider silks by both the 3ω and transient electrothermal methods. *Materials & Design, 119(7),* 22–29. DOI 10.1016/j.matdes.2017.01.057.
3. Tian, D., He, C. H., He, J. H. (2018). Macromolecule orientation in nanofibers. *Nanomaterials, 8(11),* 918. DOI 10.3390/nano8110918.
4. Tian, D., He, J. H. (2018). Self-assemble of macromolecules in a long and narrow tube. *Thermal Science, 22(4),* 1659–1664. DOI 10.2298/TSCI1804659T.

5. Tian, D., He, J. H. (2020). Control of macromolecule chains structure in a nanofiber. *Polymers, 12(10),* 2305. DOI 10.3390/polym12102305.
6. Zhou, C. J., Li, Y., Yao, S. W., He, J. H. (2019). Silkworm-based silk fibers by electrospinning. *Results in Physics, 15(44),* 102646. DOI 10.1016/j.rinp.2019.102646.
7. Yu, D. N., Tian, D., He, J. H. (2018). Snail-based nanofibers. *Materials Letters, 220(1),* 5–7. DOI 10.1016/j.matlet.2018.02.076.
8. Yu, D. N., Tian, D., Zhou, C. J., He, J. H. (2019). Wetting and supercontraction properties of spider-based nanofibers. *Thermal Science, 23(4),* 2189–2193. DOI 10.2298/TSCI1904189Y.
9. Tian, D., Zhou, C. J., He, J. H. (2019). Sea-silk based nanofibers and their diameter prediction. *Thermal Science, 23(4),* 2253–2256. DOI 10.2298/TSCI1904253T.
10. Stein, E., Vigo, C. (2017). The last woman who makes sea silk. *BBC News*.
11. Sardinia, M. P., Vigo, C. (2015). *The last woman who makes sea silk*. BBC. http://www.bbc.com/news/magazine-33691781.
12. Stein, E. (2017). The last surviving sea silk seamstress. *BBC Travel*.
13. Sumitra, C. (2015). Vigo-The world's last sea silk seamstress. Oddity Central.
14. van Huygen, M. (2015). Untangling the secrets of sea silk, the ancient mediterranean's elusive luxury textile. Mental Floss.
15. Wilhelm, M. H., Filippidi, E., Waite, J. H., Valentine, M. T. (2017). Influence of multi-cycle loading on the structure and mechanics of marine mussel plaques. *Soft Matter, 13(40),* 7381–7388. DOI 10.1039/C7SM01299C.
16. Carrington, E. (2008). Along the silk road, spiders make way for mussels. *Trends in Biotechnology, 26(2),* 55–57. DOI 10.1016/j.tibtech.2007.11.003.
17. Reinecke, A., Bertinetti, L., Fratzl, P., Harrington, M. J. (2016). Cooperative behavior of a sacrificial bond network and elastic framework in providing self-healing capacity in mussel byssal threads. *Journal of Structural Biology, 196(3),* 329–339. DOI 10.1016/j.jsb.2016.07.020.
18. Houda, J., Abbassi, H. (2019). Analysis of the influence of viscosity and thermal conductivity on heat transfer by Al_2O_3-water nanofluid. *Fluid Dynamics & Materials Processing, 15(3),* 253–270. DOI 10.32604/fdmp.2019.03896.
19. Kriraa, M., Souhar, K., Achemlal, D., Yassine, Y. A., Farchi, A. (2020). Fluid flow and convective heat transfer in a water chemical condenser. *Fluid Dynamics & Materials Processing, 16(2),* 199–209. DOI 10.32604/fdmp.2020.07986.
20. Ou, Q., Ji, P., Xiao, J., Wu, L. (2019). A study on the properties of resin transfer molding cyanate ester and its t800 grade carbon fiber composites. *Fluid Dynamics & Materials Processing, 15(1),* 27–37. DOI 10.32604/fdmp.2019.04787.
21. Lee, H., Scherer, N. F., Messersmith, P. B. (2006). Single-molecule mechanics of mussel adhesion. *Proceedings of the National Academy of Sciences of the United States of America, 103(35),* 12999–13003. DOI 10.1073/pnas.0605552103.
22. Wilhelm, M. H., Filippidi, E., Waite, J. H., Valentine, M. T. (2011). Mussel-inspired adhesives and coatings. *Annual Review of Materials Research, 41(1),* 99–132. DOI 10.1146/annurev-matsci-062910-100429.
23. Yang, Y. J., Choi, Y. S., Jung, D., Park, B. R., Hwang, W. B. et al. (2013). Production of a novel silk-like protein from sea anemone and fabrication of wet-spun and electrospun marine-derived silk fibers. *NPG Asia Materials, 5(6),* e50. DOI 10.1038/am.2013.19.
24. Ye, Y., Wu, C., Guo, B., Zhu, A., Lv, Z. (2014). Isolation and characterization of ten polymorphic microsatellite markers for the blue mussel (*Mytilus edulis*). *Biochemical Systematics and Ecology, 54,* 5–7. DOI 10.1016/j.bse.2013.12.015.
25. Li, S. G., Liu, C., Zhan, A. B. (2017). Influencing mechanism of ocean acidification on byssus performance in the pearl oyster pinctada fucata. *Environmental Science & Technology, 51(13),* 7696–7706. DOI 10.1021/acs.est.7b02132.
26. Tian, D., Zhou, C. J., He, J. H. (2019). Strength of bubble walls and the Hall-Petch effect in bubble-spinning. *Textile Research Journal, 89(7),* 1340–1344. DOI 10.1177/0040517518770679.
27. Tian, D., He, J. H. (2020). Control of macromolecule chains structure in a nanofiber. *Polymers, 12(10),* 2305. DOI 10.3390/polym12102305.

28. Li, X. X., He, J. H. (2020). Bubble electrospinning with an auxiliary electrode and an auxiliary air flow. *Recent Patents on Nanotechnology, 14(1),* 42–45. DOI 10.2174/1872210513666191107122528.
29. Li, X., Li, Y., Li, Y. (2020). Gecko-like adhesion in the electrospinning process. *Results in Physics, 16(4),* 102899. DOI 10.1016/j.rinp.2019.102899.
30. Liu, P., He, J. H. (2018). Geometrical potential: An explanation on of nanofiber's wettability. *Thermal Science, 22(1),* 33–38. DOI 10.2298/TSCI160706146L.